Journal of Solid State Chemistry 182 (2009) 2285–2289

Contents lists available at ScienceDirect

Journal of Solid State Chemistry

journal homepage: www.elsevier.com/locate/jssc

Field emission of vertically aligned V_2O_5 nanowires on an ITO surface prepared with gaseous transport

Ming-Cheng Wu, Chi-Shen Lee *

Department of Applied Chemistry, National Chiao Tung University, 1001 University Rd., Hsinchu 30010, Taiwan

ARTICLE INFO

Article history:
Received 18 March 2009
Received in revised form
13 May 2009
Accepted 27 May 2009
Available online 6 June 2009

Keywords:
Crystal growth
Nanomaterials
Optical materials and properties
V_2O_5

ABSTRACT

Growing V_2O_5 nanowires (NWs) on a conducting glass substrate combines gaseous transport and pyrolytic deposition of vanadium polyoxometalate anions, and yields vertically aligned vanadium-oxide nanowires. Scanning electron and transmission electron microscopy, selected-area electron diffraction, Raman spectra and powder X-ray analyses indicate that V_2O_5 nanowires as synthesized were single-crystalline and grew anisotropically among direction [010]. $NH_2OH \cdot HCl$ served not only as a reducing agent to produce vanadium polyoxometalate clusters but also as a source of NH_3 gas to facilitate the vapor pyrolysis and deposition. The optical properties of V_2O_5 nanowires exhibit a character dependent on structure. Field emission (FE) measurements show a small turn-on field voltage ~8.3 V/μm, maximum current density 1.8 mA/cm^2, and a linear Fowler–Nordheim behavior.

1. Introduction

Metal-oxide nanocrystals with a one-dimensional (1D) structure, such as a nanowire (NW) [1,2], nanotube [3], nanorod [4,5] or nanoribbon [6–8], show unique physical and chemical properties because of their large surface area and unique shape, which have made these materials effective for applications in photovoltaic devices [2,9,10], field emission (FE) display [3,11], etc. Among these materials, V_2O_5 exhibits a peculiar structural type and a band gap ~2.5 eV; its prospective applications include photochromic and electrochromic devices [2,10], chemical sensing [12,13], catalysis [14], and positive electrodes of rechargeable lithium battery [15,16]. The structure of orthorhombic V_2O_5 exhibits layers of a 2D network containing chains of edge-sharing VO_5 square pyramids with five-fold coordination of vanadium and oxygen atoms. Among syntheses of V_2O_5 with a 1D nanostructure are template-assisted growth [4], surfactant/inorganic self-assembly [17], *e*-beam sputtering, chemical-vapor deposition [18], pulsed laser deposition [19,20] and hydrothermal [1,3,5,17] approaches. Vertically aligned V_2O_5 nanorods are grown through template-based electrodeposition on an aluminum substrate or sol electrophoretic deposition on an ITO substrate [4], but these methods generally require polymers as template materials [1,3,11,21], the products are polycrystalline, and the conditions of electrodeposition are difficult to control.

We applied an original route of vapor pyrolysis and deposition to grow an aligned 1D nanostructure of α-MoO_3 of controlled size on a glass substrate with a water-soluble polyoxometalate compound, $(NH_4)_{12}[Mo_{36}O_{108}(NO)_4 \cdot (H_2O)_{16}] \cdot 33H_2O$ (Mo_{36}) [22]. In the use of this technique, a precursor that promotes the initial deposition of seed crystals on a substrate is a critical factor for the formation of aligned α-MoO_3 nanorods. This preparation is expected to be useful for the growth of a new metal oxide with a desired nanostructure from a suitable precursor. Here we report the deposition of vertically aligned V_2O_5 nanowires under mild conditions without template materials. The results of field emission measurements show small actuation voltages and a large current density of V_2O_5 nanowire arrays, which properties are prospectively useful in an optoelectronic nanodevice.

2. Experiments

2.1. Synthesis

V_2O_5 NWs were grown on a substrate with a method simple, economical and free of template. A mixture of V_2O_5 powder (0.4 g, Aldrich, 99.99%), $NH_2OH \cdot HCl$ (0.4 g, Fluka, 99.99%), and NH_4Cl (0.4 g, Aldrich, 99.99%) was placed in a conical flask, and stirred at 23° C. The mixture turned from orange to green, indicating the reduction of V_2O_5 [21]. This solution (1 mL) was loaded into a glass vial (volume 15 mL, external diameter 10 mm, height 50 mm), and an ITO substrate was placed on top of the vial. Before each experiment, the ITO substrate was cleaned with an organic solvent and then rinsed in deionized water. The V_2O_5 NW

* Corresponding author. Fax: +886 3 5723764.
E-mail address: chishen@mail.nctu.edu.tw (C.-S. Lee).

0022-4596/$ - see front matter © 2009 Elsevier Inc. All rights reserved.
doi:10.1016/j.jssc.2009.05.042

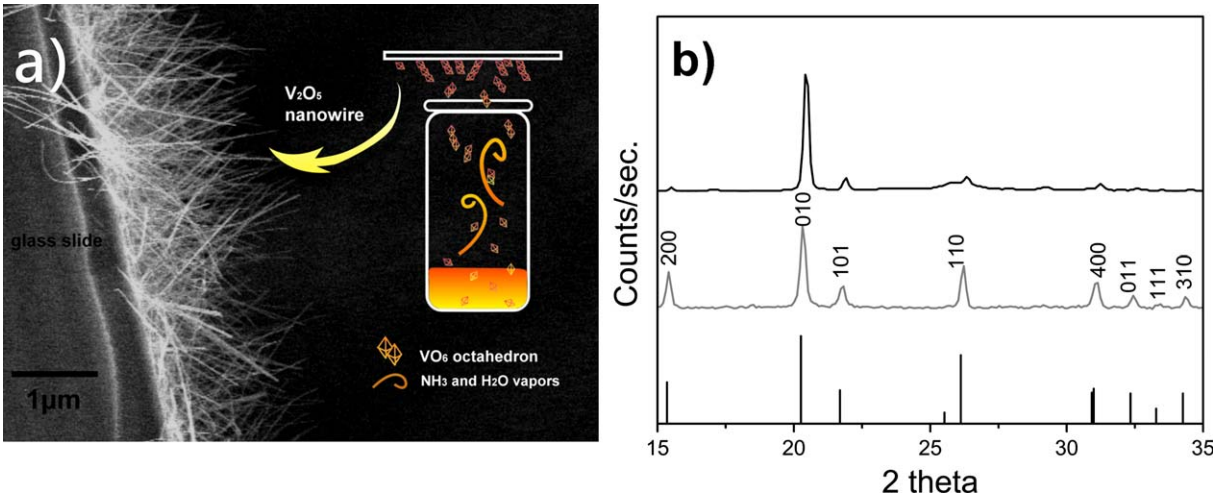

Fig. 1. (a) Schematic illustration of experiments to deposit V_2O_5 NWs on the surface of a substrate. (b) XRD profile of V_2O_5 NWs (black) as synthesized and residual V_2O_5 powder from the bottom of the reaction vessel (gray).

were grown in a horizontal box furnace; a schematic illustration appears in Fig. 1a. The temperature was raised to 320–420 °C over varied durations (0.5–2 h); the substrate in the furnace cooled naturally to 23 °C. Additional experiments show that other substrates such as a glass slide and titanium metal foil can likewise serve to deposit V_2O_5 NWs with procedures similar to those specified above. When the reaction proceeded without $NH_2OH \cdot HCl$, the V_2O_5 as synthesized exhibited irregular shapes. These V_2O_5 NWs as prepared are stable in air for several months. Under 450 °C treatment, no obvious different occur in XRD, scanning electron microscope (SEM) and the field emission test of V_2O_5 NWs on ITO.

2.2. Characterization with XRD, UV, PL, SEM, TEM and FE

The product as prepared was characterized with powder X-ray powder diffraction (XRD, Bruker AXS D8 Advance, Leipzig Germany, CuKα radiation at 40 kV and 40 mA), a scanning electron microscope (Hitachi, S-4700I, operated at 15 kV), a transmission electron microscope (TEM, JEOL, JEM-3000F, operated at 200 kV), ultraviolet and visible absorption spectra (Hitachi U-3010 spectrometer, scanning 190–1000 nm, Al_2O_3 plate as reference), photoluminescence (PL, Jobin-Yvon Spex Fluorolog-3 fluorimeter, $\lambda_{ex} =$ 365 nm, filter wavelength = 400 nm, Xe lamp, 23 °C, scanning wavelength 200–800 nm), and Raman spectra (semiconductor laser, $\lambda = 450$ nm; data were collected at 60 nm/min). Refining the maxima of the XRD patterns with least-squares fitting using the CELREF program yielded the unit-cell parameters [23]. For TEM experiments, the sample was prepared by first scraping the V_2O_5 NWs from ITO glass, followed by ultrasonically dispersing the NWs in methanol for 5 min. The resulting methanol-NWs mixture was then dispersed onto a holey carbon-coated 100 mesh copper grid. The methanol evaporated in the dry environment, leaving a distribution of NWs on the carbon film. The field emission was measured in a vacuum chamber with a pressure less than 3×10^{-7} Pa near 23 °C. The distance between the sample and electrode was adjusted to 150, 120 and 60 μm. The measurements were performed several times to obtain reproducible results.

3. Results and discussion

Fig. 1b show XRD patterns of a product as deposited on an ITO substrate and residue in the bottom of the reaction vial. Both patterns showed several reflections that were indexed to the orthorhombic V_2O_5 structure ($a = 11.513(2)$ Å, $b = 3.567(4)$ Å, $c = 4.466(5)$ Å, $V = 180.71(2)$ Å^3, *Pmmn* (No. 59)—orthorhombic, JCPDF 41-1426); no signals due to impurity phases were detected. For the product on the ITO surface, a diffraction feature at $2\theta \sim 20°$ assigned as (010) is dominant among all other signals in the pattern. The diffraction signals from the residue in the bottom of vial showed no distinct preferential orientation.

The morphology of the V_2O_5 NW as synthesized was examined with scanning and transmission electron microscopes, as shown in Fig. 2a. The side-view image clearly reveals V_2O_5 NWs that are nearly vertical aligned to the surface of the ITO substrate with no irregular particle. The highly magnified SEM image evidently shows a single nanowire containing a smooth and clean surface throughout its length (inset of Fig. 2a). The V_2O_5 wires as synthesized show ribbon-like morphology with an average width within 50–100 nm and a length up to several tens of micrometers.

The HR-TEM image taken of a portion of a nanowire revealed parallel lattice fringes with inter-layer distances ~1.109 nm (Fig. 2b), which corresponds to planes (100) of V_2O_5 in its orthorhombic phase. The SAED pattern (inset in Fig. 2b) reveals clear diffraction spots and the *d*-spacing parallel to the NW is close to 3.4 Å, indicative of the single-crystalline nature and confirming that the grown NWs are single-crystalline and grown preferentially along direction [010].

The results of investigating the effect of temperature on the growth of V_2O_5 NWs on an ITO surface are shown in Fig. 3. The results show that products from experiments at both temperatures exhibit a wire shape of V_2O_5. The average length of V_2O_5 wire deposited at 320 °C is about 10 μm, which increases to ~100 μm when the experiment was performed at 420 °C, but the widths of each nanowire are similar (~80 nm). The side-view SEM images (inset of Fig. 3a and b) indicate that the density of coverage of V_2O_5 NW is increased for the experiment at a higher temperature.

To understand how the V_2O_5 NWs were formed, we tested several conditions of thermal evaporation to discern the effect of precursor on the deposition of V_2O_5 nanomaterials on ITO glass. Without $NH_2OH \cdot HCl$ there was no growth of V_2O_5 on ITO glass at any temperature. Replacing $NH_2OH \cdot HCl$ with NH_3 (aq) or NH_4Cl in the precursor solution also yielded no sign of crystal growth on ITO glass. The presence of $NH_2OH \cdot HCl$ in the growth process was found to be essential, which is not only provide the H_2O and NH_3 vapor source, but also reduced V_2O_5 to polyvanadate species

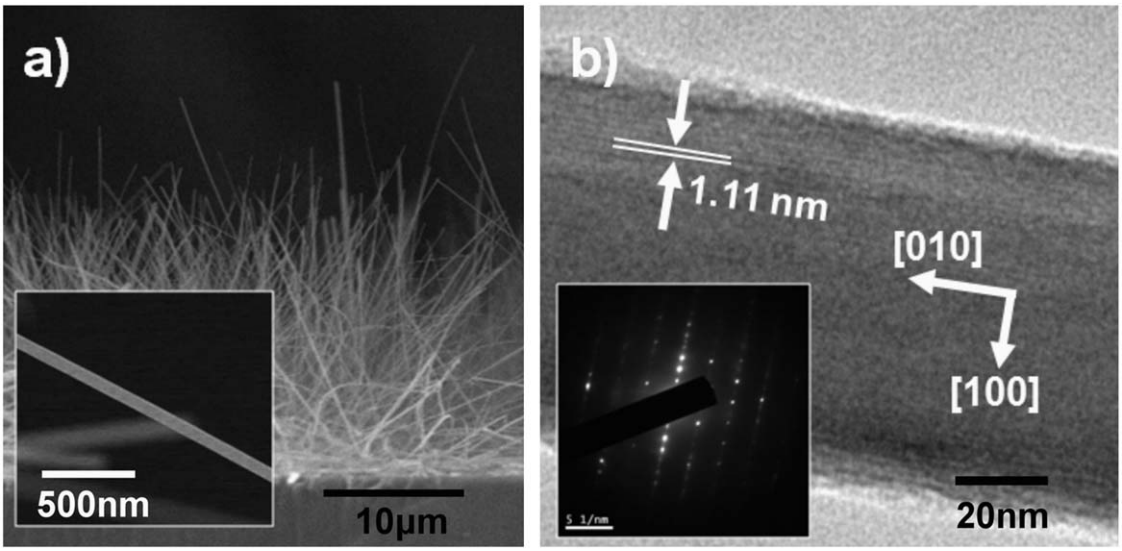

Fig. 2. SEM (a) and TEM (b) images of V_2O_5 NWs as synthesized.

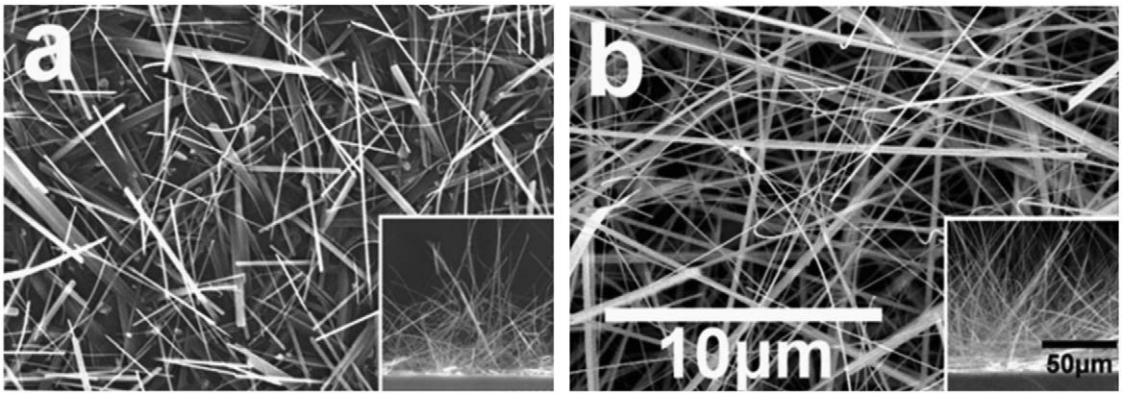

Fig. 3. SEM images of V_2O_5 NWs as synthesized, deposited at 320 °C (a) and 420 °C (b).

dissolved in solution. These results indicate that V_2O_5 NWs were not deposited directly by bulk V_2O_5 powder via gaseous transport. We demonstrated the mechanism to grow V_2O_5 NW on substrate as follows. Initially, bulk V_2O_5 powder dispersed in acid solution and was reduced by $NH_2OH \cdot HCl$ to form green solution, indicative of the formation of polyvanadate species [24]. During the process to form V_2O_5 NWs, polyvanadate species were delivered with the assistance of $H_2O(g)$ and $NH_3(g)$ (from $NH_2OH \cdot HCl$) to deposit on the surface of the ITO glass substrate through interactions between polyvanadate and –OH and –O groups of glass substrate. Upon calcination at elevated temperatures, polyvanadate species tended to crystallize, leading to the formation of nanowires. It is possible that polyvanadate species were decomposed to form clusters made up of $[VO_6]_n$ octahedra units, and then transferring to the glass surface to form V_2O_5 NWs. Accordingly, NH_3 and H_2O vapor produced on heating the solution become the carriers to assist nanocrystals of VO_x clusters to deposit on a glass substrate. The crystal growth is influenced by stacking of $[VO_6]_n$ along the anisotropic direction [010].

We measured the optical absorption and photoluminescence to elucidate the intrinsic optical properties of the V_2O_5 NWs aligned on an ITO surface. The UV–visible absorption spectrum of the films as deposited exhibits an onset of absorption near ~500 nm, indicative of a band gap near 2.48 eV (Fig. 4a), which is blue-shifted relative to bulk V_2O_5 powder (E~2.2 eV). The band gap shift is a result of defects and oxygen vacancies at the surface of V_2O_5 NWs, which is typically observed for V_2O_5 and transition metal oxide.

The luminescence properties of V_2O_5 in both bulk powder and NWs were investigated with PL spectra with the same determinate area ($0.5 \times 1\ cm^2$) and thickness (0.05 mm) for both bulk and NWs samples; the results appear in Fig. 4b. PL spectra of bulk V_2O_5 powder show a main emission band with maximum near 375 nm, whereas spectra of V_2O_5 NWs show the main band at ~500 nm as well as a band centered about 375 nm. In previous discussion of the optical properties of V_2O_5 in relation to the band structure, the emission of bulk V_2O_5 is assigned to transitions of electrons between valence (O-2p) and conduction band (V-3d). The photoluminescence of V_2O_5 NWs exhibits not only radiative transitions (~375 nm) similar to bulk V_2O_5 but also transitions between the separate band from V-3d and the O-2p band [18,25,26].

The similar emission near 375 nm for bulk and V_2O_5 NWs might be due to a removal of oxygen from the oxide lattices or reduced valence states of vanadium ions [10,20]. However, the significant difference of emission in the low energy band (~500 nm) is due to defects and oxygen vacancies at the surface of V_2O_5 NWs. Broad photoluminescence lines were reported by Díaz-Guerra's group for V_2O_5 with elongated nanostructures [18]. The emission of a V_2O_5 nanowire deposited at 420 °C is greater than at 320 °C because of the greater density of coverage and the greater length of wires.

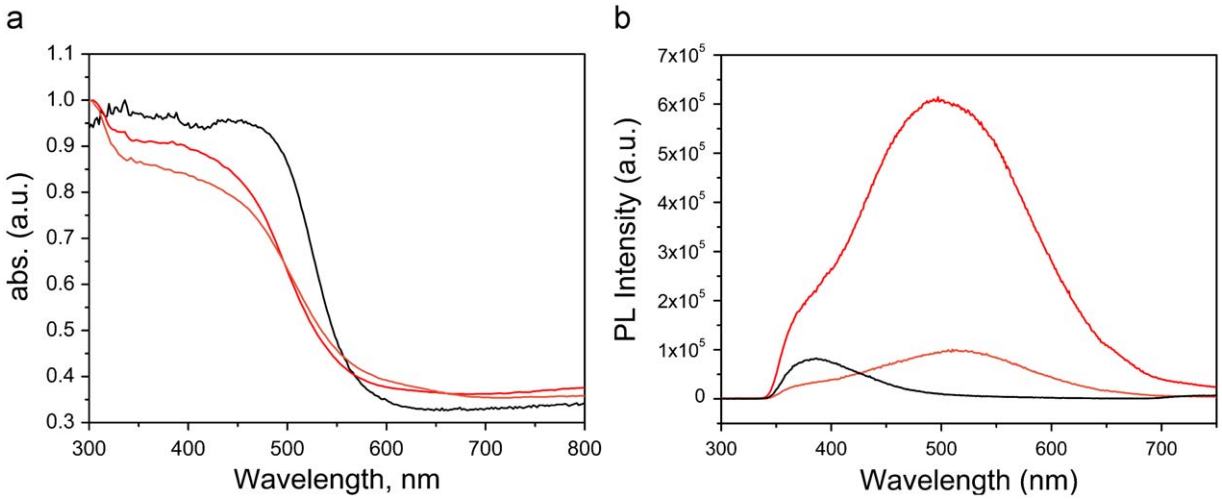

Fig. 4. (a) Diffuse reflectance spectrum of bulk V_2O_5 powder (black) and V_2O_5 NWs as synthesized, prepared at 320 °C (orange) and 420 °C (red). (b) PL spectrum for bulk V_2O_5 powder (black) and V_2O_5 NWs as synthesized, prepared at 320 °C (orange) and 420 °C (red). The black, orange and red lines are V_2O_5 samples as bulk, wire at 320 °C and wire at 420 °C, respectively.

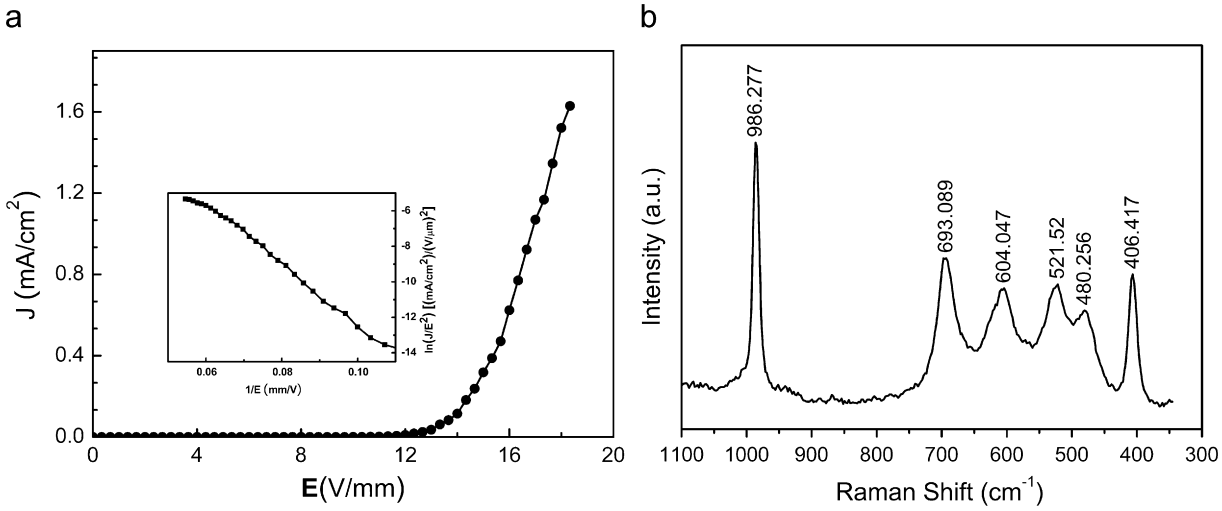

Fig. 5. (a) Emission current densities versus electric field for a sample as synthesized with an emitting surface of area 25 mm^2. (b) Raman spectrum of V_2O_5 NWs on Ti foil (red) and ITO (black) substrate.

The as-synthesized V_2O_5 NWs with vertically aligned structure may exhibit interesting field emission effect, which was measured with a parallel-plate configuration of electrodes near 295 K with a separation 100 μm between the anode and an emitting surface of area 25 mm^2. Fig. 5a shows the emission current density (J) from the V_2O_5 NW as a function of applied field (E). The turn-on field (E_{to}) is ~8.3 V/μm at a current density 10 μA/cm^2. This result is comparable to literature values for $V_2O_5 \cdot nH_2O$ and ZnO nanorod arrays [11,27]. The maximum density of emission current is 1.8 mA/cm^2 at a field ~18 V/μm, indicative of a satisfactory FE property. A Fowler–Nordheim (F–N) plot of ($\ln I/E^2$) versus ($1/E$) appears in the inset of Fig. 5a; a linear relation indicates that the field emission from the film of V_2O_5 NWs conforms to the F–N theory and the emitted current is caused by quantum tunneling at the surface [5,28]. The Raman spectrum of V_2O_5 NWs as synthesized on ITO glass, at 23 °C, exhibits the vibrational pattern shown in Fig. 5b, with lines at 995, 700, 285, 147, 525, 480 and 406 cm^{-1}, assigned to V_2O_5 in its orthorhombic phase [12,29].

4. Conclusion

We have demonstrated a deposition method simple, economical, mild and free of template to prepare vertically aligned V_2O_5 NWs in the first direct synthesis of single-crystalline vanadium-oxide nanowire with an ultralarge aspect ratio. Comprehensive structural investigations including XRD, SAED, and HREM show that the NWs comprise orthorhombic V_2O_5 in a pure phase growing along direction [001]. The ultraviolet and visible absorption spectrum reveals a semiconducting property with a band gap 2.48 eV, and measurements of field emission indicate a small actuation field ~8.33 V/μm and a large current density. The V_2O_5 NWs as deposited present a unique structure and electrical properties that might be used as a FE emitter. A possible mechanism of growth is proposed. The investigation of V_2O_5 NWs on various substrates, including ITO, glass slide, and titanium foil demonstrates significant advantages for the pyrolytic deposition, a method that might be extensible to the fabrication of other metal-oxide nanostructures with appropriately chosen

precursors and synthetic parameters. This mechanism is anticipated to be applied to fabricate various metal-oxide nanocrystals on oxide substrates with special crystal morphologies on choosing a suitable precursor.

Acknowledgments

For technical assistance we thank Dr. Hwo-Shuenn Sheu at National Synchrotron Radiation Research Center for the XRD experiment, Professor Teng-Ming Chen for UV and PL measurements, Prof. Ian Liao for Raman measurements, and Professor Hsin-Tian Chu for FE measurements. National Science Council (contracts NSC94-2113-M-009-012, 94-2120-M-009-014) supported this research.

References

[1] F. Zhou, X. Zhao, C.G. Yuan, L. Li, Cryst. Growth Des. 8 (2008) 723.
[2] K.-C. Cheng, F.-R. Cheng, J.-J. Kai, Sol. Energy Mater. Sol. Cell. 90 (2006) 1156.
[3] W. Chen, C. Zhou, L. Mai, Y. Liu, Y. Qi, Y. Dai, J. Phys. Chem. C 112 (2008) 2262.
[4] K. Takahashi, S.J. Limmer, Y. Wang, G. Cao, J. Phys. Chem. B 108 (2004) 9795.
[5] L. Mai, W. Guo, B. Hu, W. Jin, W. Chen, J. Phys. Chem. C 112 (2008) 423.
[6] L. Kong, Z. Liu, M. Shao, Q. Xie, W. Yu, Y. Qian, J. Solid State Chem. 17 (2004) 690.
[7] R. Ostermann, D. Li, Y. Yin, T. McCann, Y. Xia, Nano Lett. 6 (2006) 1297.
[8] H. Zhu, Z. Zheng, X. Gao, Y. Huang, Z. Yan, J. Zou, H. Yin, Q. Zou, S.H. Kable, J. Zhao, Y. Xi, W.N. Martens, R.L. Frost, J. Am. Chem. Soc. 128 (2006) 2373.
[9] M. Law, L.E. Greene, J.C. Johnson, R. Saykall, P.D. Yang, Nature 4 (2005) 455.
[10] S. Nishio, Chem. Mater. 14 (2002) 3730.
[11] C. Zhou, L. Mai, Y. Liu, Y. Qi, Y. Dai, W. Chen, J. Phys. Chem. C 111 (2007) 8202.
[12] S.T. Oyama, G.T. Went, K.B. Lewis, A.T. Bell, G.A. Somorjait, J. Phys. Chem. B 93 (1999) 6786.
[13] C.-J. Mao, H.-C. Pan, X.-C. Wu, J.-J. Zhu, H.-Y. Chen, J. Phys. Chem. B 110 (2006) 14709.
[14] L. Chen, B. Yang, X. Zhang, W. Dong, K. Cao, X. Zhang, Energy Fuels 20 (2006) 915.
[15] C.K. Chan, H. Peng, R.D. Twesten, K. Jarausch, X.F. Zhang, Y. Cui, Nano Lett. 7 (2007) 490.
[16] V. Protasenko, S. Gordeyev, M. Kuno, J. Am. Chem. Soc. 129 (2007).
[17] S. Shi, M. Cao, X. He, H. Xie, Cryst. Growth Des. 7 (2007) 1893.
[18] C. Díaz-Guerra, J. Piqueras, Cryst. Growth Des. 8 (2008) 1031.
[19] D. Barreca, L. Armelao, F. Caccavale, V.D. Noto, A. Gregori, G.A. Rizzi, E. Tondello, Chem. Mater. 12 (2000) 98.
[20] C.V. Ramana, R.J. Smith, O.M. Hussain, C.C. Chusuei, C.M. Julien, Chem. Mater. 17 (2005) 1213.
[21] J. Livage, Chem. Mater. 3 (1991) 578.
[22] M.C. Wu, C.S. Lee, Mater. Res. Bull. 44 (2009) 629.
[23] B. Laugier, J. Bochu, Celref, 〈http://www.inpg.fr/LMGP〉; Laboratoire des Materiaux et du Génie Physique de l'Ecole Supérieure de Physique de Grenoble.
[24] W. Yang, C. Lu, X. Zhan, H. Zhuang, Inorg. Chem. 41 (2002) 4621.
[25] A. Talledo, C.G. Granqvist, J. Appl. Phys. 77 (1995) 4655.
[26] J.C. Parker, D.J. Lam, Y.N. Xu, W.Y. Ching, Phys. Rev. B 42 (1990) 5289.
[27] X.P. Yuan, A.H. Hu, Y.M. Jiang, Y. Xu, Z. Hu, Nature Nanotechnol. 16 (2005) 2039.
[28] Q. Tang, T. Li, X.H. Chen, D.P. Yu, Y.T. Qian, Solid State Commun. 134 (2005) 229.
[29] J. Wang, K.E. Gonsalves, J. Comb. Chem. 1 (1999) 216.